

Electron Paramagnetic Resonance and Small-Angle Neutron Scattering Studies of Mixed Sodium Dodecyl Sulfate and (Tetradecylmalono)bis(*N*-methylglucamide) Surfactant Micelles

P. C. Griffiths,* A. Y. F. Cheung, G. J. Finney, and C. Farley

Department of Chemistry, University of Wales Cardiff, PO Box 912, Cardiff CF10 3TB, U.K.

A. R. Pitt and A. M. Howe

Kodak Limited R&D, Headstone Drive, Harrow, Middlesex HA1 4TY, U.K.

S. M. King and R. K. Heenan

ISIS Facility, Rutherford Appleton Laboratory, Chilton, Didcot OX11 0QX, U.K.

Barney L. Bales

Department of Physics and Astronomy, California State University at Northridge, Northridge, California 91330-8268

Received July 25, 2001. In Final Form: November 9, 2001

Small-angle neutron scattering (SANS) and electron paramagnetic resonance (EPR) have been used to characterize mixed micelles comprising the anionic surfactant sodium dodecyl sulfate (SDS) and the sugar-based nonionic surfactant (tetradecylmalono)bis(*N*-methylglucamide) (C₁₄BNMG). Parallel studies using protonated and deuterated SDS have permitted the calculation of the mole fraction of SDS in the micelle (x_{SDS}). The size of the hydrophobic core of the mixed micelles is essentially invariant with mole fraction x_{SDS} . The volume of the polar shell containing the surfactant headgroups increases with decreasing x_{SDS} . The amount of water present in this shell can be obtained from knowledge of the shell volume and the number and volume of the two types of headgroup occupying the shell. Water comprises about 70% of the polar shell in SDS but is almost completely excluded from the headgroup region of micelles of the nonionic surfactant. EPR has also been used to determine the polarity index, which contains a contribution from the OH groups on the headgroup of the sugar surfactant as well as a contribution from the water. From the rotational correlation time of the spin-probe, a microviscosity has been calculated that increases with decreasing x_{SDS} , perhaps due to steric hindrance of the large glucamide groups or hydrogen bonding between them.

Introduction

Small-angle neutron scattering (SANS) has proved to be a very powerful technique for studying the morphology of the structures formed in aqueous solution by surfactants.¹ In principle, analysis of SANS data provides information about the size and shape of the structures, as well as the interaction between them within the context of a particular model. Nevertheless, in practice, sometimes more than one physically reasonable model will fit the scattering data. Thus, it is important to seek other experimental information in order to select the best model. Recently, we have been developing and applying electron paramagnetic resonance (EPR) techniques to study mixed micelles to limit or otherwise “restrain” the SANS analysis. Of particular interest are binary surfactant mixtures of the anionic surfactant sodium dodecyl sulfate (SDS) and a series of nonionic surfactants, (*n*-alkylmalono)bis(*N*-methylglucamide)s (C_{*n*}BNMG).

Typically, binary surfactant mixtures offer improved performance and cost-effectiveness compared with single-

surfactant systems. Many of the benefits arise from nonideal phenomena associated with specific interactions between the two surfactants.² Several approaches exist to discuss the onset of micellization and composition of the mixed surfactant aggregates formed, the most widely cited being (i) the ideal mixing model of Clint,³ which has been quite successful in describing mixed systems of similar surfactants, (ii) Rubingh's⁴ very successful but largely empirical regular solution theory (RST) centered on the parameter β to account for specific interactions between the two surfactants; and (iii) the more comprehensive molecular-thermodynamic models of Blankschtein et al.⁵ and Bergstrom et al.⁶

(2) Abe, M.; Ogino, K. In *Solution Properties of Anionic-Nonionic Mixed Surfactant Systems*; Abe, M., Ogino, K., Eds.; Mixed Surfactant Systems, Surfactant Science Series; Dekker: New York, 1997.

(3) Clint, J. J. *J. Chem. Soc.* **1975**, 71, 1327

(4) Rubingh, D. N. *Solution Chemistry of Surfactants*; Plenum Press: New York, 1979.

(5) Blankschtein, D.; Shiloach, A.; Zoeller, N. *Curr. Opin. Colloid Interface Sci.* **1997**, 2, 294. Sarmoria, C. Puvvada, S.; Blankschtein, D. *Langmuir* **1992**, 8, 2690.

(6) Bergstrom, M.; Eriksson, J. C. *Langmuir* **2000**, 16, 7173. Bergstrom, M. *Langmuir* **2001**, 17, 993.

* Corresponding author. E-mail: griffithspc@cardiff.ac.uk.

(1) Pedersen, J. S. *Curr. Opin. Colloid Interface Sci.* **1999**, 4, 190.

Previously, we reported the critical micelle concentrations,⁷ along with the structural (SANS)⁹ and dynamic (EPR) characterization⁸ of binary mixtures of SDS and the nonionic surfactant (dodecylmalono)bis(*N*-methylglucamide), C₁₂BNMG, which both possess C₁₂ tails. As is found for many mixed anionic–nonionic surfactant solutions, a “synergism” was observed in the CMC behavior—the measured CMC being lower than the prediction from ideal mixing theory. The SDS/C₁₂BNMG pair is a particularly interesting system, as the size and shape of the mixed micelles vary only very slightly with composition. Thus, the mixed micelles are similar in size and shape to the two pure surfactant micelles.^{8,9,10–12} In essence, replacing an SDS molecule in the micelle by one C₁₂BNMG molecule has little effect on the structure of the micelle, except to displace a volume of solvating water comparable to the difference in the respective headgroup volumes. The dynamics are however quite different across the composition range—the addition of a C₁₂BNMG molecule substantially increases the local viscosity of the headgroup region. As part of the work on these mixed micellar systems,⁷ we also reported the CMC behavior of asymmetric systems, where the tail length of the nonionic surfactant was decreased or increased by two carbons so that it no longer “matched” that of the SDS. The system containing the longer tailed nonionic, (tetradecylmalono)-bis(*N*-methylglucamide) (C₁₄BNMG) showed an interesting switch from antagonistic behavior at low SDS solution mole fractions (α_{SDS})—i.e. the measured CMC being higher than the ideal prediction and, indeed, higher than CMC of C₁₄BNMG—to a synergistic behavior at high α_{SDS} . In this paper, we explore this feature in more detail, together with both structural and dynamic behavior.

Experimental Section

Materials. Sodium dodecyl sulfate (Aldrich) was recrystallized from ethanol until no dip in the surface tension–concentration plot could be detected around the CMC. The perdeuterated SDS (Aldrich) was not recrystallized prior to use. The nonionic surfactant (Kodak European Research, U.S. patent 5,298,191) is depicted in Chart 1. It was purified extensively with reverse-phase HPLC prior to use. All other reagents were of analytical grade and used as received. The solvent used was D₂O and H₂O in the SANS and EPR measurements, respectively.

Small-Angle Neutron Scattering. The SANS measurements were performed on the fixed-geometry, time-of-flight LOQ diffractometer (ISIS Spallation Neutron Source, Oxfordshire, U.K.) over a Q -range of approximately 0.008 to 0.22 Å^{−1}. Samples were contained in thermostated 2 mm path length, UV-spectrophotometer grade, quartz cuvettes (Hellma). All measurements were carried out at 45 °C. Experimental measuring times were between 40 and 80 min.

All scattering data were normalized for the sample transmission and incident wavelength distribution, corrected for instrumental and sample backgrounds using an empty quartz cell, and for the linearity and efficiency of the detector response. The data were put onto an absolute scale using a well-characterized partially deuterated polystyrene-blend standard sample.

(7) Griffiths, P. C.; Roe, J. A.; Jenkins, R. L.; Reeve, J.; Cheung, A. Y. F.; Hall, D. G.; Pitt, A. R.; Howe, A. M. *Langmuir* **2000**, *16*, 9983.
(8) Bales, B. L.; Ranganathan, R.; Griffiths, P. C. *J. Phys. Chem.* **2000**.

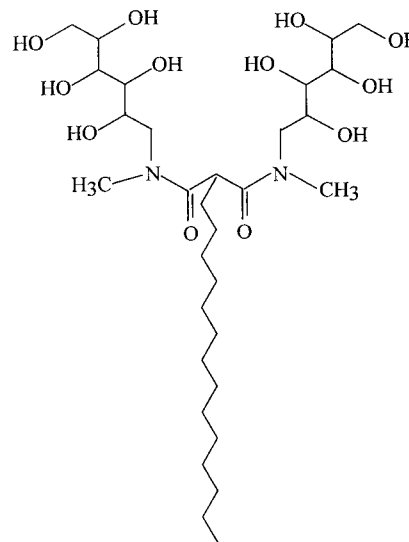
(9) Griffiths, P. C.; Whatton, M. L.; Kwan, W.; Abbott, R. J.; Pitt, A. R.; Howe, A. M.; King, S. M.; Heenan, R. K. *J. Colloid Interface Sci.* **1999**, *215*, 114.

(10) Griffiths, P. C.; Bales, B. L.; Howe, A. M.; Pitt, A. R.; Roe, J. A. *J. Phys. Chem. B* **2000**, *104*, 264.

(11) Griffiths, P. C.; Pettersson, E.; Stilbs, P.; Cheung, A. Y. F.; Howe, A. M.; Pitt, A. R. *Langmuir* **2001**, *17*, 7178.

(12) Griffiths, P. C.; Stilbs, P.; Paulsen, K.; Howe, A. M.; Pitt, A. R. *J. Phys. Chem. B* **1997**, *101*, 915.

Chart 1. Nonionic Surfactant (Tetradecylmalono)bis(*N*-methylglucamide), C₁₄BNMG



SANS Data Fitting and Analysis. The intensity of scattered radiation, $I(Q)$, as a function of the wave vector, Q , is given by

$$I(Q) = V_m^2 n_m (\rho_m - \rho_s)^2 P(Q) S(Q) + B_{\text{inc}} \quad (1)$$

where $P(Q)$ describes the morphology of the scattering species, $S(Q)$ describes the spatial arrangement of the micelles in solution, n_m is the number of micelles/unit volume, V_m is the volume of the micelle, and B_{inc} is the incoherent, background scattering. ρ is the neutron scattering length density of the micelle (subscript m) and the solvent (subscript s). The first three factors in eq 1 (viz. $V_m^2 n_m (\rho_m - \rho_s)^2$) are combined into a single parameter to “scale” the model intensity to the absolute value. With postfitting, this scalar may be recalculated using the parameters describing the micelle morphology/composition and the molar concentration of micelles to validate the fit. The calculated and observed values should lie within ~10%.

The model of the micelle adopted here is that of a charged particle with an elliptical core–shell morphology. For the SDS/C₁₂BNMG case, a rather crude version⁹ of this model was used. The elliptical core was assumed to be dodecane and its minor radius constrained to be 16.7 Å (the all-trans length of a dodecyl tail). The shell thickness and difference between the core and shell scattering length densities were the principal fitting parameters, but these are not independent. Nonetheless, an approximately linear dependence of the shell thickness on micelle composition x_{SDS} was observed. As $x_{\text{SDS}} \rightarrow 1$, the scattering length density of the shell (ρ_{shell}) tends to that of water, and the contrast ($(\rho_{\text{shell}} - \rho_s)^2$) decreases. Thus, the distinction between the shell and the continuous phase becomes poorly defined and the accuracy in determining the shell thickness drops significantly.

For the data presented here, a more refined version of the model has been employed. On the basis of the number of dodecyl and tetradecyl alkyl chains in the micelle, composition weighted-average values of the volume of the alkyl tail, volume of the polar head, and, thus, the scattering length densities of the different regions of the micelle can be calculated. However, attempts to fit the data using these averages were not successful. The fits are more consistent and the values of the parameters deduced more physically realistic when we assume that two of the CH₂ groups in the tetradecyl tail do not reside in the core region but in the shell. Thus, the core effectively comprises dodecyl tails and has a corresponding scattering length density.

The average volume/headgroup and average scattering length density of the dry headgroup region were input as constants. The values of the constants were calculated from the composition of the micelle and the values for the respective dry headgroup volumes. For the nonionic surfactant, the two –CH– linked *N*-methyl glucamides have a volume is 527 Å³, and incorporating 51 Å³ for the 2 CH₂ groups yields the total headgroup volume of

608 Å³.^{8,10} Thus, the scattering length density of the headgroup fragments of the nonionic surfactant was taken to be $\rho_{\text{nonionic}} = 1.2 \times 10^{-6} \text{ \AA}^{-2}$.

Modeling of the structure of the headgroup region of the anionic surfactant is complicated by the potential for the sodium counterions to dissociate to some degree; i.e., the degree of dissociation of sodium counterions (α_{Na^+}) may vary. If all the sodium ions are bound ($\alpha_{\text{Na}^+} = 0$), the volume of the headgroup is 74.2 Å³ and, hence, $\rho_{\text{Na sulfate}} = 3.1 \times 10^{-6} \text{ \AA}^{-2}$. If the sodium ions are completely dissociated ($\alpha_{\text{Na}^+} = 1$), the volume decreases to 60.6 Å³ and $\rho_{\text{sulfate}} = 3.8 \times 10^{-6} \text{ \AA}^{-2}$. Recent work on the closely related system SDS/C₁₂BNMG has shown that α_{Na^+} increases from $\alpha_{\text{Na}^+} = 0.27$ at $x_{\text{SDS}} = 1$ to $\alpha_{\text{Na}^+} = 0.70$ at $x_{\text{SDS}} = 0.3$; i.e., the fraction of counterions bound to the micelles is strongly dependent on the micelle composition.¹¹ It is not known how the degree of sodium ion dissociation depends on micelle composition for the SDS/C₁₄BNMG combination of surfactants. One could assume that it would not be too dissimilar to the SDS/C₁₂BNMG case. However, it is the average headgroup scattering length density and volume that are required and these are volume-weighted averages of the two surfactant headgroups present in the polar shell. Due to the much greater volume of the sugar headgroup, adopting an incorrect value for α_{Na^+} will only have a significant effect on the overall headgroup region scattering length density for SDS-rich cases. Under those conditions, α_{Na^+} must tend toward 0.27. Thus any discrepancy introduced by assuming $\alpha_{\text{Na}^+} = 0.27$ is greatly reduced. Therefore, we took a constant value of $\alpha_{\text{Na}^+} = 0.27$, corresponding to the situation for simple SDS micelles, and hence, $\rho_{\text{SDS head}} = 3.3 \times 10^{-6} \text{ \AA}^{-2}$ and volume = 70.5 Å³. The maximum error in the both the average headgroup scattering length density and average headgroup volume introduced by using this assumption occurs over the range $0.35 < x_{\text{SDS}} < 0.70$ and is less than 4%, well within experimental error.

The core and solvent scattering length densities were also taken to be constant, i.e. independent of x_{SDS} . Thus, the only fitting parameters describing the form factor $P(Q)$ are the minor radius of the ellipse representing the core of the micelle R_{core} , the ellipticity X , and the volume fraction of water in shell. The thickness and scattering length density of the hydrated shell are (re-)calculated within the analysis software, based on the fraction of water in the shell, ϕ_{water} . The fit is somewhat insensitive to this parameter since the shell consists of the hydrated headgroups and is therefore not always distinct from the continuous phase. In this work, we combine the SANS data with those from the complementary technique EPR, which can provide an independent estimate of the water in the polar shell.¹³ Some trial and error was required to find the overall best fit value of ϕ_{water} due to local minima in the least-squares fits.

The structure factor $S(Q)$ was calculated using the Hayter and Penfold model¹⁴ for spheres of a given micellar charge and ionic strength, incorporating refinements for low volume fractions and a penetrating ionic background. This $S(Q)$ also requires the hard-sphere radius, the total volume fraction of the hard spheres, and the inverse Debye length. The hard-sphere radius was allowed to vary, but the volume fraction was constrained. This method of calculating the structure factor, which assumes spherical particles, remains valid for a small degrees of micelle ellipticity, as is the case here. The ionic strength is governed by the concentrations of the unimeric SDS and the free sodium counterions of the SDS in the micelle. The last contribution may be calculated knowing the degree of dissociation of the sodium counterions, α_{Na^+} , which we have assumed to have a constant value of 0.27. Thus, the only fitting parameters in the structure-factor calculation are the charge and the hard-sphere radius.

Electron Paramagnetic Resonance. Experimental details for the EPR measurements are also identical to those described previously,⁸ and therefore, only essential details are repeated here. Stock solutions of the two surfactant solutions with spin-probe/surfactant molar ratios of 1/400 were mixed to yield compositions ranging from $x_{\text{SDS}} = 0$ to 1. These nondegassed samples were sealed with a gas-oxygen torch into melting point

capillaries which were housed within a quartz EPR tube for the measurements. The temperature was controlled to ± 0.2 K by the Bruker BVT 2000 variable-temperature unit. Five spectra were taken at X-band with a Bruker ESP-300 spectrometer.

EPR Line Shape Fitting and Analysis. The line shapes were fitted to the Voigt approximation to separate the Gaussian and Lorentzian components of the spectral lines and to locate the resonance fields of the three EPR lines to a precision of a few mG.

The (uncorrected) rotational correlation times τ_{Bu} and τ_{Cu} are computed from the overall line width of the center line ΔH_{pp^0} and the peak-to-peak heights of the three lines, V_{pp^i} , where $M_i = 1, 0$, and -1 denote the low, center, and high field lines, respectively:

$$\tau_{\text{c}}^{\text{uncorrected}} = \frac{1}{2} \Delta H_{\text{pp}^0}^{\theta} \left(\sqrt{\frac{V_{\text{pp}^0}}{V_{\text{pp}^{+1}}}} + \sqrt{\frac{V_{\text{pp}^0}}{V_{\text{pp}^{-1}}}} - 2 \right) \quad (2)$$

$$\tau_{\text{b}}^{\text{uncorrected}} = \frac{1}{2} \Delta H_{\text{pp}^0}^{\theta} \left(\sqrt{\frac{V_{\text{pp}^0}}{V_{\text{pp}^{+1}}}} + \sqrt{\frac{V_{\text{pp}^0}}{V_{\text{pp}^{-1}}}} \right) \quad (3)$$

After treatment of the inhomogeneous broadening using the procedure outlined by Bales,¹⁵ corrected rotational correlation times τ_{b} and τ_{c} may be obtained:¹⁶

$$\tau_{\text{b}} = -1.27 \times 10^{-9} \tau_{\text{b}}^{\text{uncorrected}} \quad (4)$$

$$\tau_{\text{c}} = 1.16 \times 10^{-9} \tau_{\text{c}}^{\text{uncorrected}} \quad (5)$$

The derivation of eqs 4 and 5 requires that the rotational averaging of the \mathbf{g} and hyperfine tensors be isotropic, a condition satisfied when $\tau_{\text{b}} = \tau_{\text{c}} < 3$ ns.

The separation $A+$ of the low and center lines ($M_i = +1$ and $M_i = 0$) is directly related to the polarity index $H(25^\circ\text{C})$, defined as the molar ratio of OH groups in a given volume relative to water:

$$A+ = 14.309 + 1.419H(25^\circ\text{C}) \quad (6)$$

For simple SDS solutions, $H(25^\circ\text{C})$ corresponds to the volume fraction of water in the polar shell and is therefore identical to ϕ_{water} . However, some of the 10 sugar -OH moieties per nonionic surfactant can also contribute to $H(25^\circ\text{C})$. Therefore the EPR results cannot be used to constrain the SANS fitting without making an assumption about how many of the surfactant -OH groups contribute to $H(25^\circ\text{C})$. For the SDS/C₁₂BNMG pair, we found that 7.5 -OH groups contributed to $H(25^\circ\text{C})$, independent of the SDS mole fraction x_{SDS} . Here, we prefer to optimize the ϕ_{water} independent of N_{OH} but use the value of N_{OH} as a consistency check since it must lie between 0 and 10.

Results and Discussion

Throughout this work, measurements were made at a total surfactant concentration of 25 mM. To calculate the various parameters required to set up the SANS fitting approach, the micelle composition, usually expressed as the micelle mole fraction of SDS (x_{SDS}), is required. The use of SANS for measuring micelle compositions has been elegantly demonstrated by Penfold et al.¹⁷ For mixed micelles of the same size, shape, and concentration dispersed in D₂O, the measured intensity $I(Q)$ depends on the micellar composition via the square of the scattering length density difference $(\rho_{\text{m}} - \rho_{\text{s}})^2$, and ρ_{m} depends in turn on the deuterium content of the micelle. This assumes there is no isotope effect on the micelle size and shape. The micellar composition may be conveniently extracted

(13) Bales, B. L.; Messina, L.; Vidal, A.; Peric, M.; Nascimento, O. R. *J. Phys. Chem. B* **1998**, *102*, 10347.

(14) Hayter, J. B.; Penfold, J. The structure of anionic and cationic micelles studied by small-angle neutron scattering, 1991 (unpublished work).

(15) Bales, B. L. Inhomogeneously Broadened Spin-Label Spectra. In *Biological Magnetic Resonance*; Berliner, L. J., Reuben, J., Eds.; Plenum Publishing Corp.: New York, 1989; Vol. 8; p 77.

(16) Bales, B. L.; Stenland, C. *J. Phys. Chem.* **1993**, *97*, 3418.

(17) Penfold, J.; Staples, E.; Thompson, L.; Tucker, I.; Hines, J.; Thomas, R. K.; Lu, J. R.; Warren, N. *J. Phys. Chem. B* **1999**, *103*, 5204.

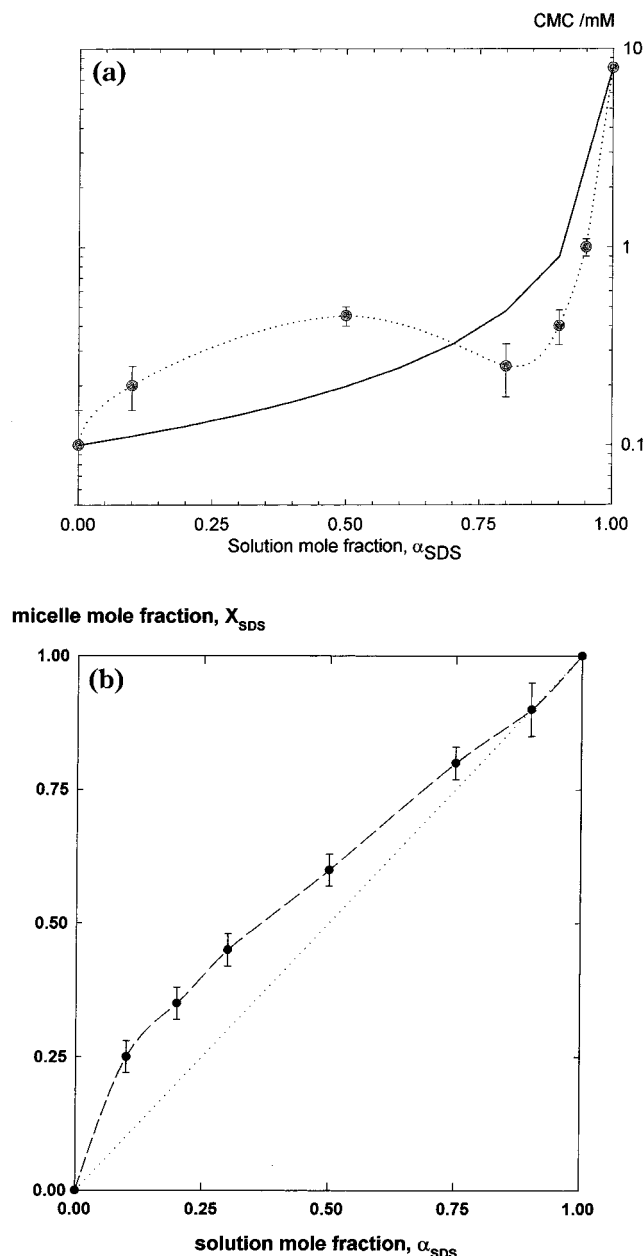


Figure 1. (a) SANS-derived micellar composition x_{SDS} of 25 mM mixed micelles comprising sodium dodecyl sulfate SDS and (tetradecylmalono)bis(*N*-methylglucamide), $C_{14}\text{BNMG}$, as a function of solution mole fraction α_{SDS} . (b) Critical micelle concentration as a function of solution mole fraction α_{SDS} . The solid line corresponds to the ideal mixing prediction.

from SANS measurements without any data fitting merely from the ratio of the scattering intensities $R(Q)$ obtained with h- and d-SDS at the same composition via

$$V_{\text{SDS}}^f = \frac{(\sqrt{R(Q)} - 1)(\rho_{C_{14}\text{BNMG}} - \rho_{\text{D}_2\text{O}})}{(\rho_{\text{h-SDS}} - \rho_{C_{14}\text{BNMG}}) - \sqrt{R(Q)}(\rho_{\text{d-SDS}} - \rho_{C_{14}\text{BNMG}})} \quad (7)$$

where

$$R(Q) = \frac{I(Q)^{\text{h-SDS}, C_{14}\text{BNMG}} - B_{\text{inc}}^{\text{h-SDS}, C_{14}\text{BNMG}}}{I(Q)^{\text{d-SDS}, C_{14}\text{BNMG}} - B_{\text{inc}}^{\text{d-SDS}, C_{14}\text{BNMG}}}$$

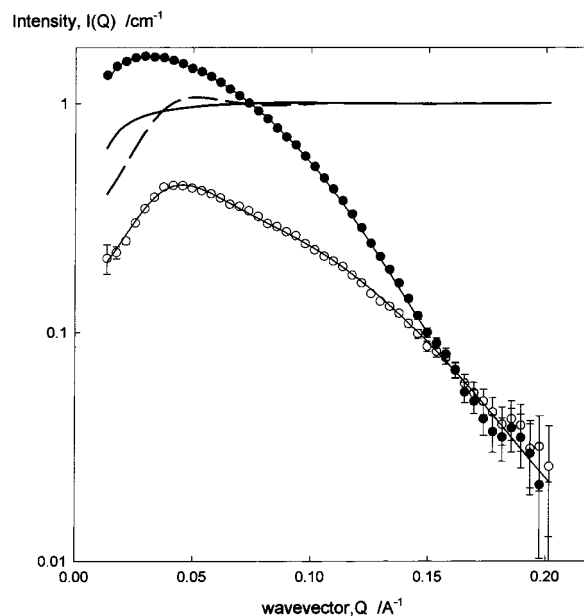


Figure 2. Intensity of scattered radiation as a function of wave vector, Q , for the two pure materials, SDS (\circ) and (tetradecylmalono)bis(*N*-methylglucamide), $C_{14}\text{BNMG}$ (\bullet), in D_2O . The solid lines drawn through the data points correspond to the fits to the constrained model as described in the text. Also shown are the structure factors $S(Q)$ for $C_{14}\text{BNMG}$ (solid line) and SDS (broken line).

The mean value of the ratio ($R(Q)$) for Q values up to $Q = 0.1 \text{ \AA}^{-1}$ is used in this calculation of x_{SDS} . The results of the analysis are shown in Figure 1a, where the micelle composition x_{SDS} is plotted in terms of the solution mole fraction α_{SDS} at a total surfactant concentration of 25 mM. Shown in Figure 1b is the CMC as a function of the solution mole fraction α_{SDS} . The two curves describe similar behavior. At low α_{SDS} , $\text{CMC}^{\text{mixture}} > \text{CMC}^{\text{ideal mixing}}$ but $x_{\text{SDS}} \approx \alpha_{\text{SDS}}$; i.e., the behavior is antagonistic. In contrast, at high α_{SDS} , the more common synergistic behavior is observed as $\text{CMC}^{\text{mixture}} < \text{CMC}^{\text{ideal mixing}}$ and $x_{\text{SDS}} < \alpha_{\text{SDS}}$.

The scattering profiles of the two simple surfactants are shown in Figure 2. The parameters defining the fits are given in Table 1. For the SDS case, the core radius (R_{core}) is found to be equivalent to the all-trans length of the dodecyl tail (16.7 Å) with a shell thickness (δ_{shell}) of 3.6 Å, comparable to other SANS studies.¹⁴ In the fitting of the profile, the charge on the micelle corresponds to a $\sim 22\%$ dissociation of Na^+ counterions, in good agreement with other studies and with our assumption of $\alpha_{\text{Na}^+} = 27\%$. The fit to the profile of the $C_{14}\text{BNMG}$ is equally good. In this case, the shell is much thicker at 7.2 Å, consistent with the greater volume of the headgroup unit (527 Å³ plus 81 Å³ for the two CH_2 groups). It is also entirely consistent with the equivalent result for the dodecyl homologue $C_{12}\text{BNMG}$ (headgroup volume 527 Å³), where the shell thickness was 6 Å.^{8,9} Most importantly, the quality of these fits provides tacit confirmation that the calculated values are physically reasonable. Also shown in Figure 2 are the structure factors pertaining to those fits. The nonionic surfactant (solid line) essentially shows a monotonic decay in $S(Q)$ as Q tends to zero, representing a soft, virtually uncharged repulsive interaction. As found with the SDS/ $C_{12}\text{BNMG}$ case, the hard sphere $S(Q)$ alone could not describe the low Q scattering. The SDS structure factor (broken line) shows the expected damped oscillatory form associated with electrostatically interacting systems.

Equally good fits are observed for the various mixed systems with deuterated/protonated SDS combinations.

Table 1. Sodium Dodecyl Sulfate (SDS)/(Tetradecylmalono)bis(*N*-methylglucamide) SANS Analysis and Constrained Core–Shell Fit, Adjusting Water Content To Obtain the Best Fit

α_{SDS}	$x_{\text{SDS}} \pm 0.02$	aggregation no. ± 5	$V_{\text{core}} \pm 500/\text{\AA}^3$	$V_{\text{shell}} \pm 1000/\text{\AA}^3$	$\delta_{\text{shell}} \pm 0.2/\text{\AA}$	$R_{\text{core}} \pm 0.1/\text{\AA}$	ellipticity ± 0.1	hard sphere radius $\pm 0.5/\text{\AA}$	scattering length density of the hydrated shell $\pm 0.1/10^{10} \text{ cm}^{-2}$	shell water vol fraction ± 0.02	$N_{\text{OH}} \pm 2$	$\alpha_{\text{Na}^+} \pm 0.05$
h-SDS												
0.00	0.00	70	24 000	43 000	7.3	16.7	1.2	33.5	1.7	0.10	5	n/a
0.10	0.25	80	28 000	41 000	6.9	16.7	1.4	27.5	2.1	0.18	4	0.45
0.20	0.35	85	29 000	46 000	7.0	16.7	1.5	27.0	2.9	0.28	2	0.40
0.30	0.45	85	29 000	41 500	6.4	16.7	1.5	29.0	3.1	0.30	2	0.35
0.50	0.60	85	29 500	36 500	5.8	16.7	1.5	29.5	3.6	0.38	4	0.30
0.75	0.80	70	23 500	23 000	4.5	16.7	1.2	23.0	4.4	0.50	6	0.25
0.90	0.90	85	29 500	25 000	4.3	16.7	1.5	23.0	5.2	0.65	6	0.20
1.00	1.00	75	25 500	18 000	3.6	16.7	1.3	19.5	5.5	0.72	0	0.25
d-SDS												
0.10	0.25	75	26 500	43 500	7.0	16.7	1.4	30.5	2.6	0.22	2	0.40
0.30	0.45	80	27 500	39 000	6.3	16.7	1.4	29.0	3.1	0.30	4	0.35
0.50	0.60	70	25 500	29 000	5.5	16.7	1.2	30.0	3.6	0.38	4	0.35
0.75	0.80	70	24 000	23 500	4.5	16.7	1.2	28.5	4.4	0.50	6	0.25

Examples are given in Figure 3a for $\alpha_{\text{SDS}} = 0.5$ and Figure 3b for $\alpha_{\text{SDS}} = 0.1$. As shown in Table 1, for all of the different anionic–nonionic mixed compositions, the same model of the micelle fits data sets obtained with both h/d contrasts, once the difference in the core scattering length density has been accounted for. This inherently confirms that only a single micelle type exists in these solutions rather than two micelle types each rich in one of the two components.

The shell thickness (δ_{shell}) decreases monotonically with increasing x_{SDS} , Figure 4a, while the core radius (R_{core}) and, hence, aggregation number are essentially invariant with x_{SDS} (Table 1). The dependencies of core radius and shell thickness on micelle composition are very similar to those observed in the SDS/C₁₂BNMG case.⁹ However, a discrepancy in aggregation number arises: our work using time-resolved fluorescence quenching TRFQ yields $N_{\text{agg}} \approx 45$ for simple SDS micelles,⁸ while SANS gives $N_{\text{agg}} \approx 70$. This is commonly found when comparing different experimental approaches¹⁸ and may arise through the different estimates of mean size each technique is sensitive to. TRFQ gives the number concentration of micelles, while SANS measures a volume-squared weighted size (eq 1). Hence, for systems with any polydispersity, the aggregation number from TRFQ will be lower than that calculated from the mean size measured by SANS. However, it is the trend in aggregation number with composition that is important when discussing variations in micelle properties. These trends are well-reproduced in SDS micelles¹⁸ irrespective of the technique used.

In the calculation of the ionic strength, we have assumed that 27% of the sodium ions are dissociated from the micelle surface. From the charge on the micelle extracted from the fit (Table 1), a derived value of α_{Na^+} can be calculated [(charge per micelle)/($N_{\text{agg}}x_{\text{SDS}}$)]. For $x_{\text{SDS}} < 0.5$, the assumption of $\alpha_{\text{Na}^+} = 0.27$ is rather crude. The discrepancy between the assumed and recalculated values of α_{Na^+} is significant. From the calculated charge on the micelle, we can see that the degree of sodium counterion binding/SDS molecule in the micelle is not constant over the whole mole fraction range and increases at low x_{SDS} , Figure 4b. A similar observation has been made by electrophoretic magnetic resonance EMR¹¹ for the SDS/C₁₂BNMG system, and those results are also shown in Figure 4b. If the degree of dissociation is greater than

0.27 (i.e. α_{Na^+} underestimated), the real ionic strength and, hence, screening length will be greater. This in turn dampens the electrostatic interaction between the micelles, leading to a low estimate for the charge on micelle. For example, refitting the $x_{\text{SDS}} = 0.2$ data set using an estimate for α_{Na^+} derived from the SDS/C₁₂BNMG system, $\alpha_{\text{Na}^+} = 0.6$, leads to a charge on the micelle of 13e rather than the tabulated value of 11e. On the basis of this value for the charge, $\alpha_{\text{Na}^+} = 0.7$, in better agreement with the initial estimate of $\alpha_{\text{Na}^+} = 0.6$. Unless α_{Na^+} is known from a separate experiment, no further interpretation should be made. However, assuming either $\alpha_{\text{Na}^+} = 0.27$ or taking the SDS/C₁₂BNMG value of α_{Na^+} at the corresponding composition does not invalidate the main conclusion expressed here that α_{Na^+} increases as x_{SDS} decreases.

Clearly, the sodium ion and sulfate headgroup prefer to be fully dissociated and hydrated but such an arrangement would lead to a significant unfavorable electrostatic interaction between adjacent headgroups over the micelle surface. This repulsion is screened by that fraction of sodium ions bound to the micelle surface. However, as the headgroups become more separated with decreasing SDS mole fraction, the fraction of sodium ions required to screen the electrostatic repulsion decreases. Alternatively, since the concentration of Na⁺ in the sample is less, the activity of Na⁺ associated with the micelle is reduced to be in equilibrium with the activity in the aqueous phase. Either way, α_{Na^+} increases with decreasing x_{SDS} . However, for the lowest micelle mole fraction studied in the SDS/C₁₂BNMG case ($x_{\text{SDS}} = 0.13$), α_{Na^+} appears to show a sudden drop in value. This could be due to dehydration of the headgroup region with the consequence that there is insufficient water to solvate the sulfate ions. In contrast, no equivalent decrease in α_{Na^+} was found for the SDS/C₁₄BNMG at a similarly low value of x_{SDS} . Whether or not the latter system might show a decrease at an even lower x_{SDS} is an interesting question, so clearly further measurements are required in the low mole fraction region. Perhaps, it should also be remembered that the above conclusions are drawn from two very different measurement techniques, so further work should be done to compare the techniques. Given that other measurements show the behavior of SDS/C₁₂BNMG and SDS/C₁₄BNMG systems to be similar, it is encouraging to see that the two techniques give similar data and trends for the two systems in Figure 4b.

The polarity index $H(25^\circ\text{C})$, linearly related to the hyperfine coupling constant, is shown in Figure 5a as a

(18) Quina, F. H.; Nassar, P. M.; Bonilha, J. B. S.; Bales, B. L. *J. Phys. Chem.* **1995**, *99*, 17028.

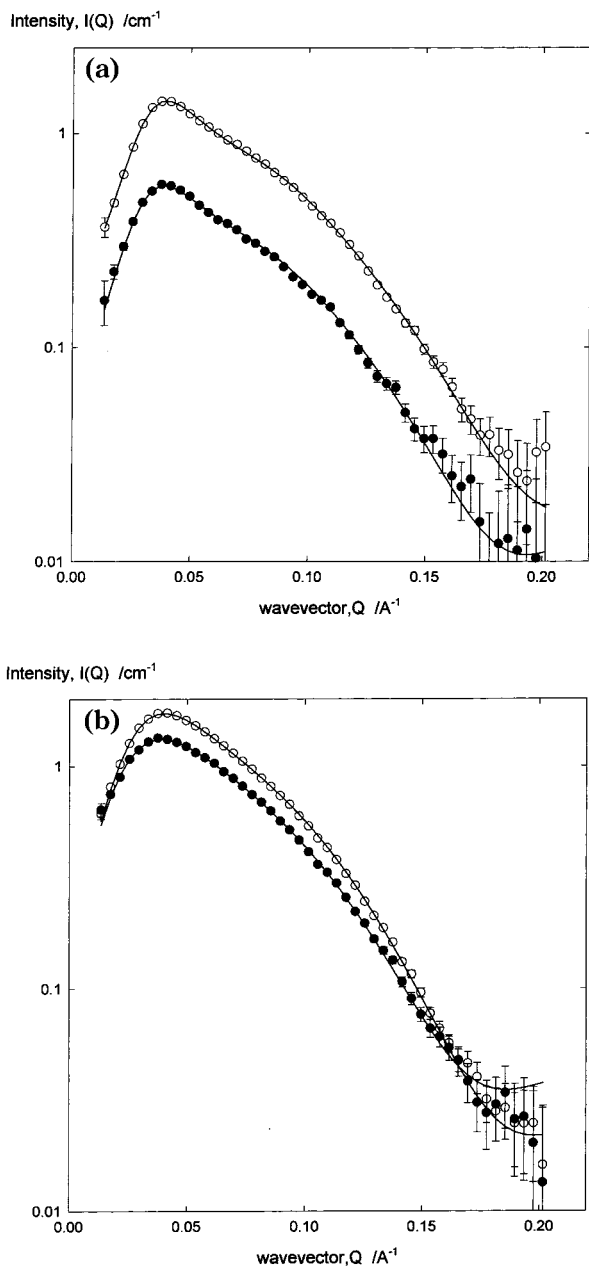


Figure 3. (a) Intensity of scattered radiation as a function of wave vector, Q , for mixed sodium dodecyl sulfate (SDS)/(tetradecylmalono)bis(*N*-methylglucamide) (C_{14} BNMG) micelles with composition $\alpha_{\text{SDS}} = 0.5$ for h-SDS (\circ) and d-SDS (\bullet) in D_2O . The solid lines correspond to fits to the constrained model as described in the text. (b) Intensity of scattered radiation as a function of wave vector, Q , for mixed sodium dodecyl sulfate (SDS)/(tetradecylmalono)bis(*N*-methylglucamide) (C_{14} BNMG) micelles with composition $\alpha_{\text{SDS}} = 0.1$ for h-SDS (\circ) and d-SDS (\bullet) in D_2O . The solid lines correspond to fits to the constrained model as described in the text.

function of SDS micelle mole fraction x_{SDS} . Also shown for comparison is the SDS/ C_{12} BNMG case.⁸ The polarity index increases with the mole fraction of SDS above $x_{\text{SDS}} \sim 0.2$ for both cases as more water is pulled into the headgroup region due to the much smaller sulfate headgroup. Over the region of composition $0.3 < x_{\text{SDS}} < 0.8$, the two sets of data are reasonably parallel with the SDS/ C_{14} BNMG curve lying well above that of the SDS/ C_{12} BNMG one. For a given micellar composition within this region, the shell thickness δ_{shell} for SDS/ C_{14} BNMG micelles is greater than that of SDS/ C_{12} BNMG and accordingly there is more water associated with the surfactant headgroups.

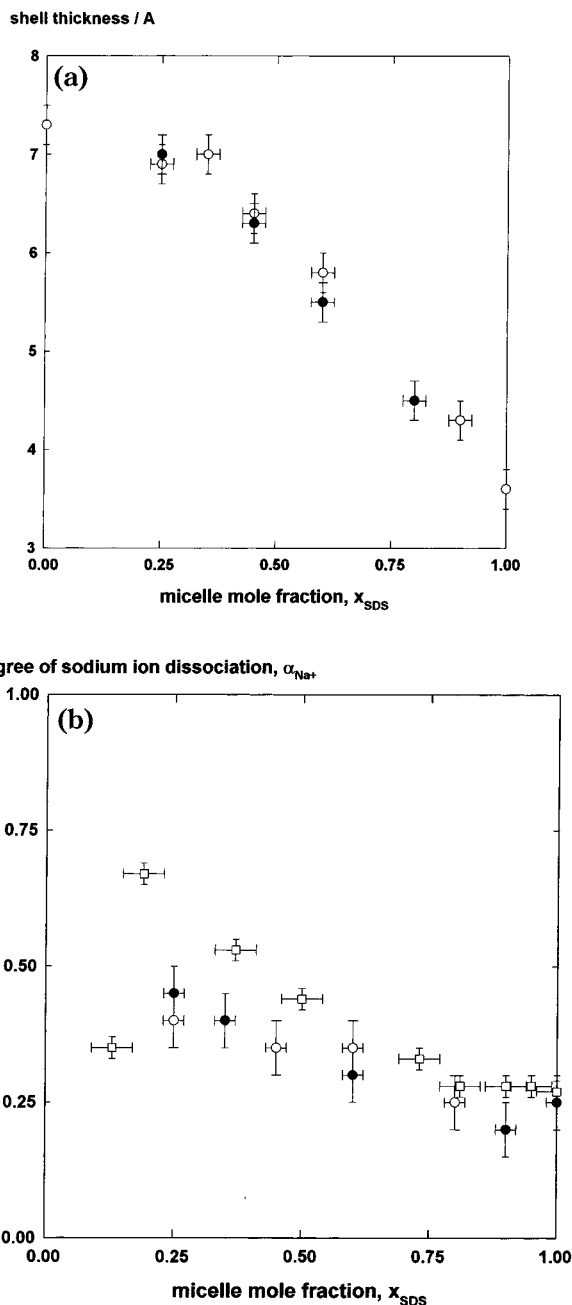


Figure 4. (a) SANS-derived shell thickness for (\circ) h-SDS/ C_{14} BNMG and (\bullet) h-SDS/ C_{14} BNMG binary mixtures as a function of micellar composition x_{SDS} of 25 mM mixed micelles comprising sodium dodecyl sulfate, SDS, and (tetradecylmalono)bis(*N*-methylglucamide), C_{14} BNMG. (b) Degree of sodium ion dissociation α_{Na^+} as a function of SDS micelle mole fraction x_{SDS} for SDS in 50 mM mixed micelles of SDS/(tetradecylmalono)bis(*N*-methylglucamide), C_{14} BNMG (SANS results; h-SDS, \circ ; d-SDS, \bullet), and SDS/(dodecylmalono)bis(*N*-methylglucamide), C_{12} BNMG (electrophoretic NMR results from ref 11, \square).

The polarity index is dependent on the water present in the headgroup region and the $-\text{OH}$ groups on the sugar. From the SANS analysis, ϕ_{water} is obtained as a fit parameter. It may also be calculated from eq 8,

$$\phi_{\text{water}} = [V_{\text{shell}} - N_{\text{agg}}\{x_{\text{SDS}}V_{\text{SDSheadgroup}} + (1 - x_{\text{SDS}})V_{\text{sugarheadgroup}}\}]/V_{\text{shell}} \quad (8)$$

where V_{shell} is the volume of the shell and $N_{\text{agg}}x_{\text{SDS}}V_{\text{SDSheadgroup}} + (1 - x_{\text{SDS}})V_{\text{sugarheadgroup}}$ corresponds to the volume occupied by the headgroups.

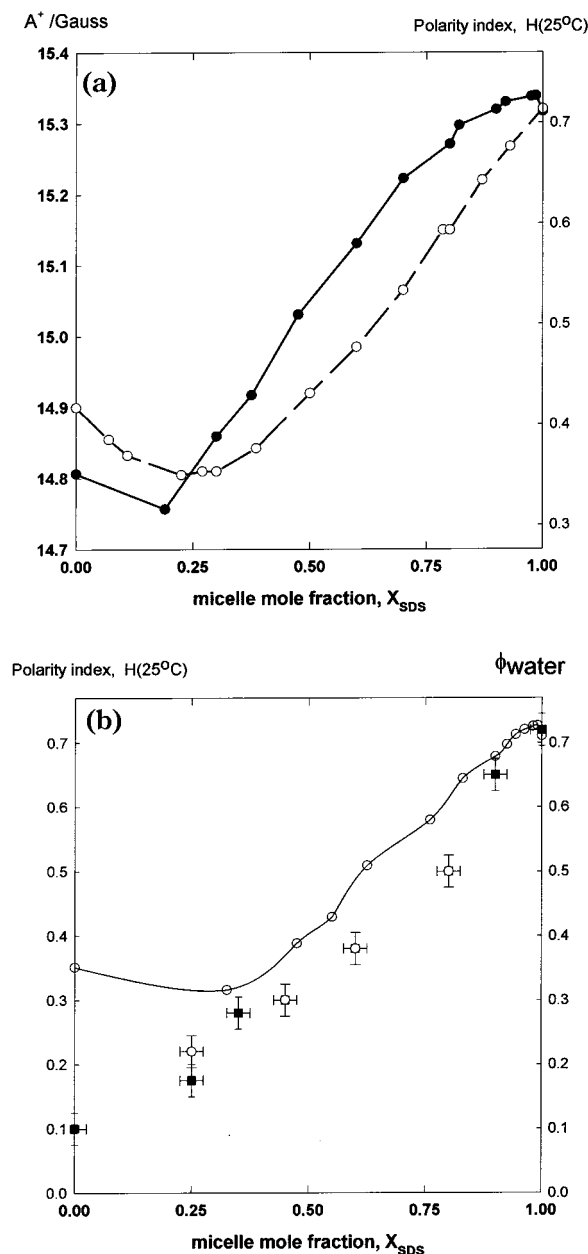


Figure 5. (a) EPR-derived polarity A^+ and linearly-related polarity index $H(25^\circ\text{C})$ of mixed micelles comprising sodium dodecyl sulfate, SDS, and (tetradecylmalono)bis(*N*-methylglucamide), C₁₄BNMG (●), and sodium dodecyl sulfate, SDS, and (dodecylmalono)bis(*N*-methylglucamide), C₁₂BNMG (○), as a function of micelle composition x_{SDS} . (b) EPR-derived polarity index $H(25^\circ\text{C})$ (○) and SANS-derived shell water volume fraction ϕ_{water} (●) of mixed micelles comprising sodium dodecyl sulfate, SDS, and (tetradecylmalono)bis(*N*-methylglucamide), C₁₄BNMG, as a function of micelle composition x_{SDS} .

This formulation is similar to that defining $H(25^\circ\text{C})$, from which the number of $-\text{OH}$ groups, N_{OH} , on the nonionic surfactant contribution to $H(25^\circ\text{C})$ may be estimated:

$$H(25^\circ\text{C}) = [V_{\text{shell}} - N_{\text{agg}}\{x_{\text{SDS}}V_{\text{SDSheadgroup}} + (1 - x_{\text{SDS}})V_{\text{sugarheadgroups}} + (1 - x_{\text{SDS}})V_{\text{H}_2\text{O}}N_{\text{OH}}\}] / V_{\text{shell}} \quad (9)$$

Here each $-\text{OH}$ group has the same effective volume as a single water molecule, $V_{\text{H}_2\text{O}} = 30 \text{ \AA}^3$. Remember, N_{OH} must lie between 0 and 10.

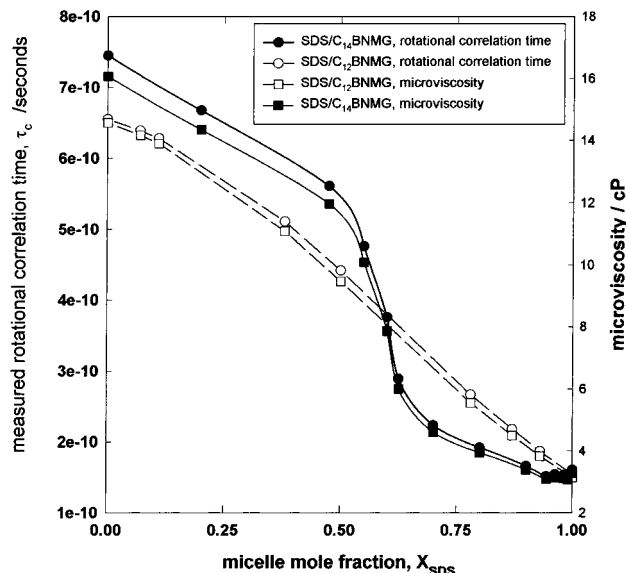


Figure 6. EPR-derived rotational correlation time τ_c (circles) and, via eqs 10–12, microviscosity (squares) of mixed micelles comprising sodium dodecyl sulfate, SDS, and (dodecylmalono)bis(*N*-methylglucamide), C₁₂BNMG (open symbols), and sodium dodecyl sulfate, SDS, and (tetradecylmalono)bis(*N*-methylglucamide), C₁₄BNMG (closed symbols), as a function of micelle composition x_{SDS} .

Figure 5b compares the dependence of the polarity index $H(25^\circ\text{C})$, which depends on the volume fraction of $-\text{OH}$ groups (water plus sugar), on the mole fraction of SDS with the volume fraction of water in the shell region ϕ_{water} . The upturn in $H(25^\circ\text{C})$ at low x_{SDS} is not seen for ϕ_{water} , indicating that over this region the $-\text{OH}$ groups contribute more to $H(25^\circ\text{C})$ than the small amount of water present. A similar conclusion was drawn from the work on SDS/C₁₂BNMG.⁸ As with the SDS/C₁₂BNMG system, N_{OH} had a value of ≈ 7 at x_{SDS} values up to ~ 0.8 . Above $x_{\text{SDS}} = 0.8$, $N_{\text{OH}} \approx 10$ within experimental error, indicating that all the OH groups on the sugar head are in the environment experienced by the spin-probe.

The measured mobility ($1/\tau_{\text{measured}}$) of the micelle-solubilized spin-probe, 16-doxy stearic acid methyl ester (16-DSE) is a combination of the mobility of spin-probe within the micelle, with correlation time (τ_{relative}) and the overall, much slower tumbling of the micelle itself, characterized by τ_{micelle} . These two processes are independent and can be separated via

$$\frac{1}{\tau_{\text{measured}}} = \frac{1}{\tau_{\text{micelle}}} + \frac{1}{\tau_{\text{relative}}} \quad (10)$$

Assuming that tumbling corresponds to the slowest motion of the micelle, τ_{micelle} may be calculated from eq 11 using the SANS data for $R_{\text{micelle}} = X^{1/3}R_{\text{core}} + \delta_{\text{shell}}$:

$$\tau_{\text{micelle}} = \frac{4\pi\eta_{\text{water}}R_{\text{micelle}}^3}{3kT} \quad (11)$$

Here η_{water} is the bulk viscosity of water.

On the other hand, τ_{relative} is determined by the local dynamics and structure of the micelle:

$$\tau_{\text{relative}} = \frac{4\pi\eta_{\text{local}}R_{\text{probe}}^3}{3kT} \quad (12)$$

Here η_{local} corresponds to a local or “microviscosity” and R_{probe} is a parameter that describes the effective hydro-

dynamic radius of the spin-probe. For 16-DSE, a value for R_{probe} of 3.75 Å has been found over a wide range of viscosities by varying water/methanol solvent composition and/or temperature.⁸ This is obviously not the actual size of the probe molecule but the effective size based on the microdynamics, a point that is discussed extensively, and validated, in ref 8.

The measured rotational correlation time (τ_{measured}) and the microviscosity (η_{local}) of the spin-probe are shown in Figure 6 for both the SDS/C₁₂BNMG and SDS/C₁₄BNMG binary mixtures. With decreasing SDS mole fraction, the values of these parameters increase for both surfactant combinations. The increase in microviscosity is probably due to steric hindrance arising from the bulky sugar headgroups, which may experience significant interglucamide hydrogen bonding. Since these micelles do not change size or shape significantly with x_{SDS} and the overall tumbling of the micelle contributes little to the measured rotational correlation times, the transformations described by eqs 11 and 12 have little effect on the shapes of the curves obtained. The microviscosity of the shell of simple C₁₄BNMG micelles is greater than that of C₁₂BNMG, which is rather surprising as both headgroup regions are similar in structure and contain very little water. The larger C₁₄BNMG micelle has a greater headgroup volume, but its aggregation number is somewhat higher. The first few molecules of nonionic surfactant to enter the SDS micelle have a far more pronounced effect on the microviscosity for the SDS/C₁₂BNMG case than for the SDS/

C₁₄BNMG case, the latter showing a constant microviscosity down to $x_{\text{SDS}} = 0.8$. This is also reflected by the greater number of OH groups contributing to $H(25\text{ }^\circ\text{C})$ for the C₁₄ nonionic surfactant at $x_{\text{SDS}} > 0.8$.

Over the composition range $0.3 < x_{\text{SDS}} < 0.8$, the microviscosity of SDS/C₁₄BNMG micelles is less than that of SDS/C₁₂BNMG, consistent with the higher fraction of water in the headgroup region. However, the SDS/C₁₄BNMG microviscosity is also more sensitive to x_{SDS} , presumably because the C₁₄BNMG micelles have a higher microviscosity than C₁₂BNMG micelles.

Conclusions

SANS and EPR have been used to study the structure of mixed anionic/nonionic surfactant micelles of SDS/C₁₄BNMG. An elliptical core-shell morphology was found to describe the SANS data. The shell thickness decreases monotonically with mole fraction of SDS in the micelle (x_{SDS}), but the core radius was invariant with x_{SDS} at 16.7 Å. Accordingly, the aggregation number of the mixed micelles does not vary with composition. At low x_{SDS} , the sugar headgroups occupy the majority of the headgroup region and the microviscosity of this region is rather high. At high x_{SDS} , the smaller sulfate headgroup results in a thinner headgroup region but one with a significantly greater volume fraction of water. Accordingly, the microviscosity is much lower at high x_{SDS} .

LA011163J